Modelling shear viscosity of soft plant cell suspensions

Cassandre Leverrier, Giana Almeida, Gérard Cuvelier, Paul Menut

Université Paris-Saclay, INRAE, AgroParisTech, UMR SayFood, 91300, Massy, France.

Abstract

Fruit purees are concentrated suspensions of highly deformable, non-spherical particles. These particles are delimited by a plant cell wall and filled with the continuous phase. They can shrink under stress, as it occurs with the increasing concentration in particles, making difficult the determination of their real volume fraction and the understanding of their rheological properties. Usually, the rheological behavior of plant suspensions is described by three concentration domains. We show here on apple puree that beside the complexity of such system, the concentration dependence of the viscosity can be described by one single model over the full range of concentration investigated. The model, originally developed for soft colloids, fits accurately the experimental results obtained on ground purees of several particle size distributions (either monomodal or bimodal) and in several continuous phases. It considers the particles stiffness and asphericity, but also highlight the effects of the continuous phase properties, for example through lubrication.

Nomenclature

C	Polymer concentration	η_{rel}	Relative viscosity
ϕ_{app}	Apparent volume fraction	η	Apparent viscosity
k_0	Specific volume of polymer in diluted solution	η_0	Continuous phase's viscosity
V	Voluminosity	a	First parameter of Batchelor's equation

C_i	Insoluble solids concentration	b	Second parameter of Batchelor's equation
ϕ	Volume fraction (generical term)	$[\eta]$	Intrinsic viscosity
λ	Huggins parameter	C^*	Overlapp concentration
k	Mendoza's equation parameter	C_i^*	Critical concentration in apple particle suspensions
ϕ_c	Critical volume fraction	ϕ_{rcp}	Random close packing volume fraction
α	Mendoza's equation first parameter	β	Mendoza's equation second parameter
r	Radius of the core of star polymer particle	R	Radius of the entire star polymer particle
S	Current model fitting parameter	Λ	Spreading of the sigmoid
ϕ_i	Volume fraction reached at the inflection point of the sigmoid	σ	Distribution width
ϕ_{max}	Maximum attainable volume fraction		

Introduction

Food products include many examples of soft materials: emulsions (mayonnaise, milk...), foams (chocolate mousse, Chantilly, whipped egg white...), suspensions (spreadable paste, processed fruits and vegetables...) and gels (yoghurt, jelly ...). Most of them are complex multicomponent systems, which explains the rapid expansion of the application of physics and materials science in food science and technology[1–4]

Fruit and vegetable purees consist in a suspension of plant cells and are an example of soft material encountered in food. They are obtained by cooking and grinding the flesh of a fruit or a vegetable. Flesh is composed of cells, whose size varies according to the plant, from tens to several hundreds of microns. A plant cell wall, mainly composed of insoluble polymers, delimits the cells. During cooking, soluble polymers (pectins) contained in the

middle lamella between the cell walls will solubilize and the fruit flesh disintegrates, releasing cell clusters of heterogeneous size, individual cells and cell fragments. Cooking parameters will have an impact on the particle size distribution and on the rigidity of the walls, an intensive cooking leading to more porous and less rigid cell walls, and less cell clusters in suspension. Fruit or vegetable suspensions are thus composed of a dispersed phase, the plant particles (plant cells without turgor), suspended in an aqueous continuous phase mainly composed of water, polymers (pectins), sugar and ions initially present in the fruit or vegetable.

Plant particles obtained thereby have specific structural and physical properties. They are only made of plant cell walls filled with the continuous phase, thus defining a particle whose volume varies with the concentration of the suspension[5,6]. These particles are porous, deformable and compressible and can be nested in each other. Plant particles are large size non-colloidal objects, which shape and rigidity depend on plant's variety and maturity, but also on mechanical or thermal treatments undergone by the fruits. Shape and rigidity also depend on particle's internal structure: clusters of cells are larger but also more irregular in shape and more rigid than individual cells, due to their internal architecture[6].

Suspensions of plant particles strongly resemble soft glassy materials[7], which in rheological terms are defined as "very soft solids, yet flow readily above a critical yield stress"[8]. The category of soft glassy material comprises foams, emulsions and star polymer gels among others. Specifically, the suspensions of plant particles could be part of the soft particle glasses, defined by Seth (2011) as "materials made of deformable particles as diverse as microgels, emulsion droplets, star polymers, micelles and proteins which are jammed at volume fraction where they are in contact and interact via soft elastic repulsions", behaving like "weak elastic solids at rest but flow[ing] very much like liquids above the yield stress".

Understanding the rheological behavior of such suspensions and mastering parameters impacting this behavior is a challenge for the food industry. If the rheology of plant particle suspensions has been extensively studied in order to understand the impact of many parameters such as variety, thermal and mechanical treatments or the continuous phase [10,11] no rheological model applicable over a wide range of concentrations has been

developed yet to describe the rheological behavior of such suspensions, in flow or at rest. In general, models for the viscosity of granular or colloidal suspensions require the knowledge of the particle volume fraction, which is here difficult to estimate. Literature does not agree on one definition so far and many parameters are still used to evaluate the medium's congestion such as the insoluble solids content[6], the water insoluble solids content[12] or the percentage of pulp[13]. Nevertheless, three concentration domains have been highlighted on several kind of plant particle suspensions[5,6,14] and discussed in literature. Until now, their modelling have been limited to empirical equations, such as linear, exponential or power law fittings, which range of validity is limited to their own concentration domain.

In this article, we will propose a single model describing the viscosity as a function of the concentration over the full range of concentration investigated, taking into account the compression when the concentration increases. This model will be conceptually based on a model initially proposed by Mendoza[15,16] for soft particles, and initially applied to star polymers. We propose here to adapt this model so that it can describe the viscosity divergence that occurs at a finite, maximum volume fraction above which particles cannot be compressed anymore. The validity of the model will be tested on real apple purees characterized by different particles properties, so that it will be possible to correlate the model parameters with particles properties such as their rigidity, shape and size. We will investigate how the effect of polydispersity, associate with different values of the random close packing volume fraction, affect the quality of the model. Finally, we will use a single suspensions of monodispersed apple particles suspended in several continuous phases to evaluate how the model parameters could also reflect variations in continuous phase lubrication properties.

Material and methods

Plant material and processing conditions

A single batch of mature Golden Delicious (*Malus domestica* Borkh. cv Golden Delicious) was transformed into puree by a French manufacturer (Conserves France) following an industrial hot break process. From this raw material, two kinds of suspensions were studied: ground

purees and model suspensions made of isolated apple cells dispersed in various aqueous media.

Ground purees

Three particle size distributions were obtained using mechanical treatment as described in Leverrier et al. (2016). By using such procedure, and by contrast with thermal treatments cell walls' rigidity is not affected by grinding. The architecture of the particle (either individual cells or clustered) may however have an impact on its global rigidity: clusters are supposed to be more rigid when compared to individual cells[6].

Model suspensions

Model suspensions composed of individual cells were also constructed from the same raw material using wet sieving and solvent exchange as described in Leverrier (2017). This protocol is known to maintain an intact cell structure[18]. Apple particles (isolated dry individual cells) were suspended in three controlled aqueous media (one solution of NaCl at 1%w/w and two solutions of carboxymethylcellulose of 1%w/w and 3.2%w/w, of 1mPa.s, 12.6mPa.s and 108mPa.s respectively) and in the original continuous phase of apple puree obtained by centrifugation (apple serum of 12.8 mPa.s).

Particle size distributions and rheological measurements

The particle size distribution of samples was obtained using a laser diffraction analyser (Mastersizer 2000, Malvern Instruments). Samples were dispersed in distilled water (refractive index: 1.33). The refractive index of vegetable cells is estimated to be 1.52 and the absorption was set at 0.1[6,10,17,19,20]. Measurements were made in triplicate. Microscopic observations were made as described in Leverrier et al. (2016).

The rheological measurements were performed using a stress controlled rheometer (MCR301, Anton Paar) equipped with large gap coaxial cylinders[6,17]. Apparent viscosities of the suspensions were taken at $50s^{-1}$.

Results & Discussion

How to access the particles' volume fraction?

Unlike hard spheres, the volume fraction of soft deformable particles is not well defined[21,22]. For microgel suspensions, the apparent volume fraction is often linearly related to the polymer concentration C [23] and based on the particles' volume in diluted conditions[21], for which polymer networks are in their most swollen state. The apparent volume fraction of microgels suspensions is thus frequently defined as $\phi = k_0 C$, where k_0 is their specific volume in diluted conditions[21], determined from an Einstein-type equation.

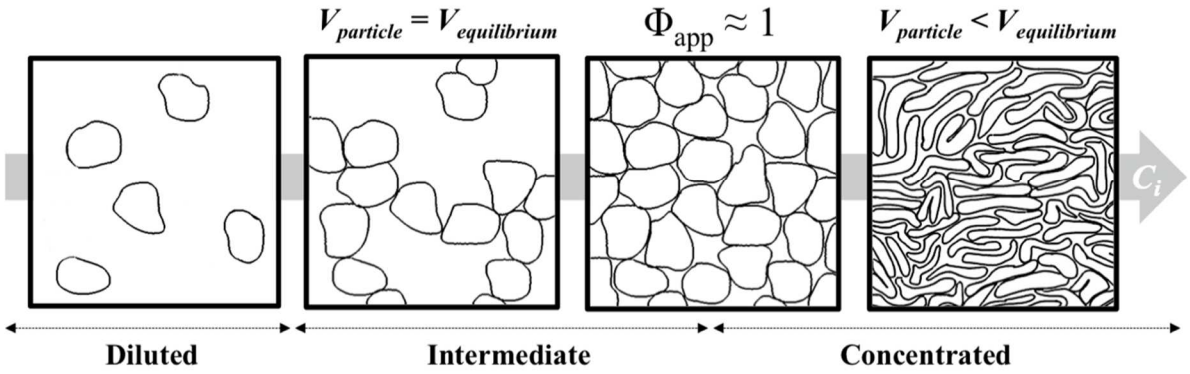

Figure 1. Schematic representation of the impact of the concentration on the particles shape and size adapted from Leverrier et al. (2017).

A comparable approach has been used in 2012 by Espinosa (2012) on apple cells suspended in their own serum. The volume fraction of individual apple cells can be then written as

$$\phi_{app} = V C_i \quad (1)$$

Where V is the *voluminosity* of the cells (volume occupied by unit of mass) and C_i is the insoluble solids content. The parameter V being linked to the particle size and shape. By integrating Eq. (1) in a second order expression of the kind of Batchelor & Green (1972) such as $\eta_{rel} = \frac{\eta}{\eta_0} = (1 + a\phi + b\phi^2)$, and by analogy with the Huggins equation (defined for dilute polymer solutions as $\frac{\eta_{rel}-1}{C} = [\eta] + \lambda[\eta]^2$ the following equation was obtained :

$$\frac{\eta_{rel} - 1}{C_i} = aV + bC_iV^2 \quad (2)$$

152

153 The parameter a is linked for spherical particles to their deformability, its value is between
154 1 (for gas bubbles)[25] and 2.5 (hard spheres). Relying on the work of Nawab & Mason
155 reported in Macosko (1996), $a = 1.7$ was used for individual apple cells[20]. Their *voluminosity*
156 was then determined from viscosity measurements on diluted suspensions, allowing to
157 define the apparent volume fraction of apple cells suspensions as $\phi_{app} = 1.3C_i$.

158

159 This approach provides access to ϕ_{app} and takes into account the deformability and the
160 rigidity of the particles by setting the parameter a. However, it slightly overstates the real
161 volume fraction occupied in intermediate and concentrated domains.
162 Indeed, considering a linear relationship between the volume fraction and the quantity of
163 cell wall in suspension (insoluble solids content C_i) implies that the *voluminosity* of the
164 particles is the same whatever the concentration. This is not the case, as illustrated in Figure
165 1. Three concentration domains were highlighted in literature[5,14]. In the diluted domain,
166 particles are able to flow freely and do not interact with each other. In the intermediate
167 domain, described as the building of a stress-bearing network between particles, particles
168 are at rest in contact with each other: elastic properties become measurable. Note that for
169 spherical particles, the onset of the intermediate domain is usually referred as random loose
170 packing, it occurs at volume fractions which could be much below random close packing, and
171 depend on cohesive and frictional interactions[27,28]. Finally, the concentrated domain
172 corresponds to a domain where particles highly deform and decrease their volume to fit the
173 available space and to be able to flow.
174 It is therefore necessary to consider the particle compressibility in determining their volume
175 fraction at a given concentration.

176

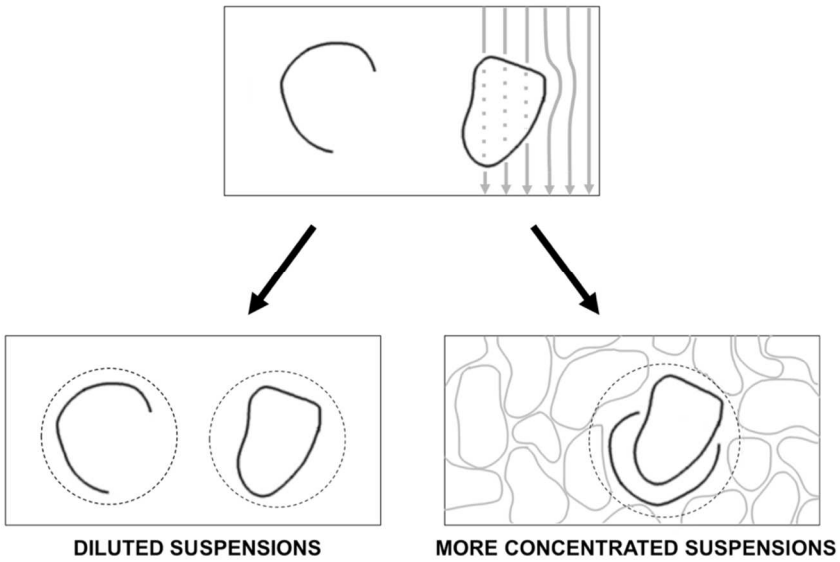

Figure 2. Schematic representation of two of the plant particles specificities: cell wall porosity allows a (limited) flow through the particle (up), and presence of cell fragment allow particles interlocking in concentrated suspensions. Both phenomena may result in lower hydrodynamic volumes than expected.

The presence of cells fragments also restricts the use of a linear relationship between volume fraction and insoluble solid content. If plant particle suspensions are composed of cell walls having maintained their cell integrity, cell fragments are also present in the suspension. In diluted domain, cell fragments occupy a hydrodynamic volume comparable to the one of an entire cell (Figure 2). In contrast, in intermediate or concentrated domains, their hydrodynamic volumes may be significantly lower than the ones occupied by entire cells (Figure 2). Thus, if the insoluble solids content is the same, the hydrodynamic volume occupied by cell fragments in diluted or in more concentrated domains can be strongly different.

The apparent volume fraction of soft particles can also be evaluated by defining the volume fraction as the ratio of the concentration to a critical concentration. This approach is widely used in polymers' rheology where the apparent volume fraction occupied by the polymers is often defined as $\phi_{app} = {C}/{C^*}$, where C^* is the overlap concentration of polymers[15,16]. The overlap concentration is obtained using the polymer molecular weight and the radius of the sphere equivalent, considering the particles dimensions as if they were hard spheres[15,16]. It is worth noting that this approach allows volume fractions greater than 1, due to the

possible interpenetration of particles[15] and that it allows to distinguish the concentration domains.

A similar approach was applied on plant particles by Day et al. (2010) on carrot cells' and broccoli cells' suspensions, and by Leverrier et al. (2016) on apple cells' suspensions. For plant particles suspensions, the critical concentration is determined as a regime change in dynamic[10] or flow[6,17] properties of the suspensions when the particle concentration is increased. It corresponds to the concentration at which the particles fill all the available space and from which the particles begin to squeeze[6], represented in Figure 1 as $\phi_{app} \approx 1$. Both on carrot, broccoli and apple cell suspensions[6,10,17] this approach highlights concentration domains and materializes the transition between the intermediate and concentrated domains, thus defining a relevant parameter to evaluate the volume fraction of plant particle suspensions.

Following this approach, we define the apparent volume fraction of plant particles as:

$$\phi_{app} = \frac{C_i}{C_i^*} \tag{3}$$

where C_i is the insoluble solids content of the suspension and C_i^* is the critical insoluble solids content at the intersection between the intermediate and concentrated domains[17], obtained from rheological measurements.

Presentation of the model

Here, the proposed modelling of plant particle suspension viscosity is based on a previous work from Mendoza & Santamaría-Holek (2009) which showed that the viscosity of colloidal particles suspensions can be modelled by :

$$\eta(\phi) = \eta_0 \times \left(1 - \frac{\phi}{1 - k\phi}\right)^{-[\eta]} \tag{4}$$

where η_0 is the continuous phase viscosity, $[\eta]$ is an exponent without unit which can be assimilated to the intrinsic viscosity of the suspension (specific viscosity of the suspension for $\phi \to 0$), and k is defined as follow:

$$k = \frac{1 - \phi_c}{\phi_c} \tag{5}$$

Where ϕ_c is the critical volume fraction defined as the maximum volume fraction that can be reached by the system.

This expression takes into account the excluded volume and hydrodynamic interactions, and has been shown to fit with high accuracy suspensions of hard spheres[29], droplets[30], arbitrarily-shaped hard particles[31] or rigid core-shell permeable particles[32]. However, Eq. (4) did not apply to very soft particle suspensions[16], able to decrease their volume or to interpenetrate. Considering suspensions of star polymers and other soft particles, Mendoza[16] suggested that a critical volume fraction greater than ϕ_{rcp} (volume fraction at random close packing) may be reached since the particles can interpenetrate, and he proposes that the critical volume fraction follows :

$$\phi_c = \phi_{rcp} + \beta\phi^{\alpha} \tag{6}$$

where α and β are two adjustable parameters without unit.

This gradual increase of the critical volume fraction with the current volume fraction of the suspension, that is associated with increasing levels of particles compression, is undoubtedly the major innovation of this model.

For spherical and permeable particles, Mendoza[16] defined the intrinsic viscosity $[\eta]$ as :

$$[\eta] = \frac{5}{2}\left(\frac{r}{R}\right)^3 \tag{7}$$

where r and R are the respective radius of the (impermeable) core and the entire particles, considering a shell-permeable periphery of thickness $R - r$.

This model, that was conceived for soft particles and applied to star polymers suspensions, is intended primarily to describe the shear viscosity of colloidal-size particles suspensions. Such models can however often be applied to non-colloidal (granular-scale) systems, as commonly done for the Krieger's equation[33] for example[16,34,35].

However for plant particles, Eq. (7) cannot be used as such since particles are not spherical in shape. Moreover, the solvent permeability of the plant particles concerns the entire cell wall, and not only a surrounding area. Instead of $[\eta]$, we chose here to use a more general parameter S, which value may vary with the particle Sphericity (or Shape), Softness, Surface irregularities and Size distribution of the suspension. Using in addition the apparent volume fraction of the particles as given by Eq. (3), the initial model from Mendoza therefore becomes:

$$\eta(\phi_{app}) = \eta_0 \times \left(1 - \frac{\phi_{app}}{1 - \left[\frac{1 - \phi_{rcp} - \beta\phi_{app}^{\alpha}}{\phi_{rcp} + \beta\phi_{app}^{\alpha}} \right] \phi_{app}} \right)^{-S} \quad (8)$$

In the following sections, we will first demonstrate that this model can be successfully applied to plant suspensions. To facilitate interpretations of the model parameters, we will first set the value of ϕ_{rcp} at 0.637, corresponding to the random close packing fraction of monodisperse hard spheres[16]. We are aware that this is not fully appropriate since our system is heterogeneous in size and not spherical in shape but we used it as a first approach. The impact of the polydispersity of apple cell suspensions on ϕ_{rcp} value will also be discussed. Then, we will study the impact of the continuous phase on the parameters of the model. And finally, we will propose some adjustments to the current model.

Validation of the model

First, the effect of the particles properties on the model parameters will be evaluated. To do so, we will compare three different suspensions, characterized by different size distributions but also different particles properties (in terms of rigidity and shape). Second, we will evaluate how the volume fraction at random closed packing, ϕ_{rcp}, which depends on the sample polydispersity, affects the quality of the fit. Third, we will evaluate the impact of the continuous phase, which does not impact particles intrinsic properties but can affect frictional interactions through lubrication.

Impact of the particle size distribution

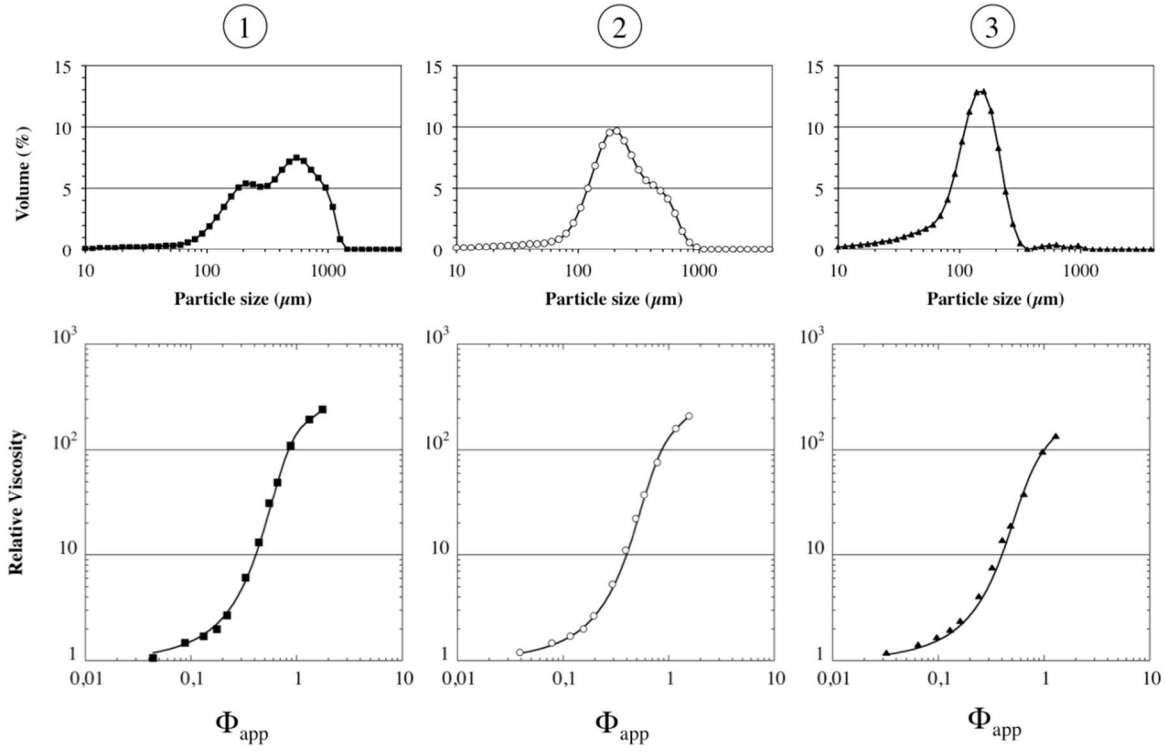

Figure 3. Modelling using Eq.(8) for three apple purees varying in particle size distributions. Data were taken from Leverrier (2016)[6]. Particle size distributions are represented on the upper side. Relative viscosity is represented as a function of the apparent volume fraction on the bottom side. Black squares, circles and black triangles stand for experimental data and the solid lines represent the modelling.

It is noteworthy that the model presented in Eq. (8) describe remarkably well the data (Figure 3) for the three purees investigated. Two purees present a bimodal particle size distributions: they contain in different proportions both very large particles up to 1000 µm

(clustered cells[6,11]) and smaller particles of about 150 µm (individual cells[6,11]), and one puree presents a monomodal size distribution, centered on 150 µm.

Table 1. Fitting parameters of the model used for the Figure 3 with $\phi_{rcp} = 0.637$.

	β	α	S	ϕ_{rcp}	R^2
(1)	0.913 (0.017)	2.100 (0.014)	3.697 (0.039)	0.637	0.999
(2)	1.035 (0.039)	2.131 (0.024)	3.893 (0.072)	0.637	0.999
(3)	1.177(0.074)	2.160 (0.031)	3.929 (0.109)	0.637	0.999

Fitting parameters used in Figure 3 are itemised in Table 1. They all increase when the average particle size decreases. However, the decrease in global particle size also reflects the presence of particles of different kind in the medium, as illustrated in Figure 4. Large particles are clusters of cells, irregular in shape and quite rigid thanks to their complex architecture. Small particles are individual cells, more regular and spherical in shape, and probably less rigid due to their purely liquid content. Grinding thus induces a decrease in particle size, but also an increase of particle sphericity and a decrease of their rigidity and their surface irregularities, which are difficult to decorrelate.

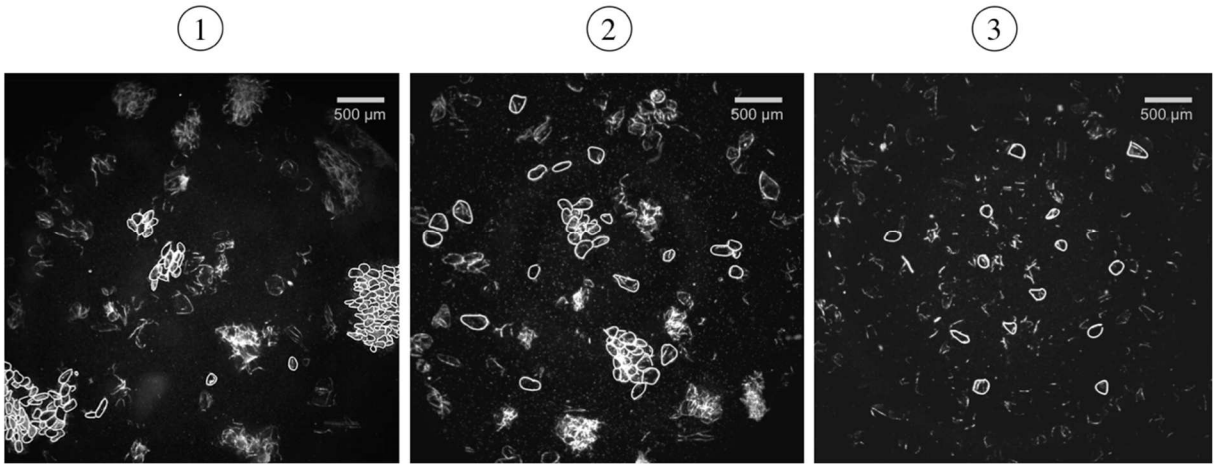

Figure 4. Microscopic observations of the three particle size distributions. Some of the particles have been highlighted to facilitate reading.

The fitting parameters α, β, and S depend on the suspension properties, and are therefore link to the particles physical properties. In the following, we investigate how their value depend on the particles rigidity and shape.

β values here obtained are 0.913, 1.035 and 1.177 respectively for the purees (1), (2) and (3). In the work of Mendoza (2013)[16], β is related to the particle deformability: the softer is the particle, the greater is β: β values between 0.244 and 0.966 were observed for 128 arms and 32 arms star polymer particles, respectively. This is consistent with our results, in which we observe that the higher the proportion of large clusters, the lower the value of β. Indeed, the complex architecture of clusters could generate a greater overall rigidity of the particle[6], thus here also β is higher when the particles are softer (smaller particles in our case). It is noteworthy that the β values of individual cells are much higher than the softer star polymer ones (with only 32 arms), while stiffer cells clusters exhibit a closer β value confirming that plant particles are highly deformable objects.

Regarding α, the values obtained on the apple purees (2.10-2.16) are slightly higher than those obtained on star polymer suspensions[16] (1.9-1.74 for 128 and 32 arms particles, respectively). In the case of star polymer suspensions, α decreases when particle deformability increases, while we observe here the opposite effect, the greatest value of α being obtained for the puree (3).
We hypothesize that this may be related to the sphericity of the particles or to their surface irregularities. Indeed, on apple purees, when the particle size decreases, the deformability increases, but surface irregularities are decreased and particle sphericity increases. However, in star polymer suspensions, the opposite effect could be anticipated: Indeed, star polymer particles with many arms are very close to hard spheres. If the number of arms decreases, particle deformability increases but particle sphericity could only be reduced, thus possibly increasing surface irregularities.

Regarding S, we observe that it increases when the particle size decreases and the deformability increases. This is similar to the r/R parameter evolution in star polymer suspensions[16] which was previously associated with particle permeability.

It should be noted that S is consistently above 2.5, while in existing models for spherical and deformable particles, the power parameter is often presented as equal to[16] or less than 2.5[25,36,37]. Higher values of the Einstein coefficient were however reported for non-sperical

particles[38]. This high value of S determined with plant particles could therefore be due to their non-spherical shape.

It is noteworthy that Eq. (8) offers, to our knowledge for the first time, the possibility to describe the viscosity dependence towards concentration of complex, non-colloidal suspensions of soft particles. The good agreement of the model with experimental data is due to the use of a critical volume fraction that evolve with the actual concentration of particles (Eq. (6)). In other words, due to their compressibility, the *effective* volume fraction of the particles do not increase as the insoluble solids content does.

Impact of the random close packing volume fraction

Up to here, the maximum packing volume fraction was taken as 0.637 for all fittings, the random close packing value for monomodal hard spheres. The impact of polydispersity on this type of highly deformable non-spherical particle suspensions was evaluated. To do so, a similar approach to the one used by Shewan *et al.* (2015)[21] on agar microgel suspensions was used. Based on the particle size distribution of our suspensions, we determined the distribution's width $\sigma = ln\frac{d_{4,3}}{d_{3,2}}$. Using the results obtained by Farr *et al*. (2009)[39], we determined the random close packing volume fraction of each suspensions, based on their polydispersity. We obtained ϕ_{rcp} values of 0.715, 0.705 and 0.70 for the purees (1), (2), (3) respectively.

Then, we determined the new model parameters in each case, they are itemized in Tableau 2. As one can see, no significant improvement is noted on the fit quality, and the impact of the particle size distribution on the parameters α, β and S remains the same as discussed in previous section. The impact of polydispersity on the maximum volume fraction seems to be negligible when modelling the data. These results are consistent with observations made in our previous work[17]: Particles having non-spherical shapes and high surface irregularities dominate the global rheological properties of suspensions, and polydispersity effect is almost negligible. For the sake of simplicity, the value of ϕ_{rcp} corresponding to monodisperse spheres $\phi_{rcp} = 0.637$ will thus be used for the rest of this work.

Tableau 2. Fitting parameters of the model used for the Figure 3 considering the particle size distribution effect on ϕ_{rcp}.

	β	α	S	ϕ_{rcp}	R^2
(1)	0.914 (0.021)	2.285 (0.018)	3.880 (0.042)	0.715	0.999
(2)	1.053 (0.044)	2.292 (0.028)	4.057 (0.072)	0.705	0.999
(3)	1.223(0.081)	2.309 (0.035)	4.090 (0.105)	0.70	0.999

Impact of the viscosity of the continuous phase

In this section, model suspensions of individual apple cells varying in continuous phase viscosity and composition will be considered (data taken from Leverrier *et al.* (2017)[17]). Such suspensions are composed of the same batch of particles, characterized by a monomodal distribution, centered on 180 µm (Figure 5). It allows us to assume that all particles have the same deformability, sphericity, surface irregularities and polydispersity, and to investigate here more specifically how a phenomenon like lubrication, which depends on the continuous phase properties, could affect the suspension viscosity other the full range of volume fraction investigate. Figure 6 represents the resulting fittings of Eq. (8) on these suspensions varying only in continuous phase. It is noteworthy that Eq. (8) fits again quite well the data, whatever the continuous phase composition.

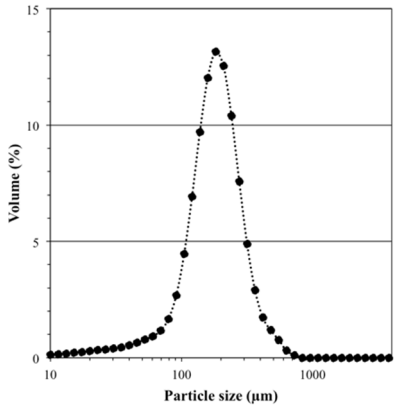

Figure 5. Particle size distribution of monomodal model suspensions.

Fitting parameters are itemised in Table 3. We observe that when the continuous phase viscosity increases, β and α increase and S decreases.

Table 3. Fitting parameters of the model used for the Figure 6.

	$\eta_0(mPa.s)$	β	α	S	ϕ_{rcp}	R^2
$NaCl$ 1%	1	0.774 (0.023)	1.989 (0.041)	4.362 (0.114)	0.637	0.997
CMC 1%	12.6	0.869 (0.036)	1.937 (0.045)	3.341 (0.095)	0.637	0.996

Apple serum	12.8	0.851 (0.016)	1.964 (0.022)	3.226 (0.043)	0.637	0.999
CMC 3.2%	108	1.222 (0.089)	2.143 (0.077)	2.621 (0.078)	0.637	0.994

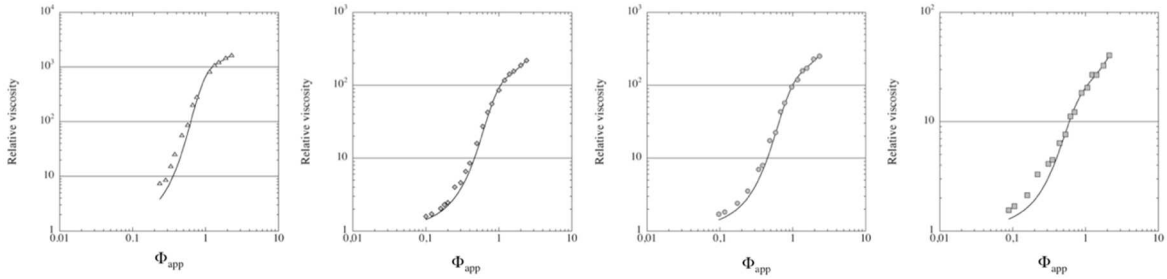

Figure 6. Modelling using Eq. (8) for model suspensions in 4 different continuous phases. Symbols represent experimental data for model suspensions, in NaCl 1% (triangles), apple serum (diamonds), carboxy-methyl-cellulose solution at 1% (circles) and carboxy-methyl-cellulose solution at 3.2% (squares). Solid lines represent the fittings resulting from Eq. (8) for each continuous phase.

Previously, and in agreement with Mendoza's approach, we have shown that α and β parameters were related to particles' deformability and sphericity (or surface irregularities). At a first look, it might seem surprising that the continuous phase composition impacts the model parameters, however, we remind here the reader that apple cells are granular, non-brownian particles. In such suspensions, frictional forces play a key role in rheological properties[40–42]. One additional consequence is that these particles are not sensitive to the depletion effects that can be observed in colloidal systems.

The increase of α with the increasing continuous phase viscosity could be due to a lubricating effect[17]. By increasing the viscosity of the continuous phase or the presence of polymers in the medium, frictions between particles are decreased.

This lower friction could have an impact on apparent surface irregularities, leading to an apparent more spherical shape of the particles. The increase of β with the viscosity of the continuous phase could be related to crowd effects. Indeed, in all cases, the viscosity of the continuous phase has been increased by introducing polymers in the continuous phase. These polymers, whose concentration increases with the continuous phase viscosity, have an intrinsic volume and thus occupy space in the medium. If the rheological properties of the suspensions are predominantly driven by the particles[6,17], the presence of polymers in the continuous phase can force particles to deform to a greater extent, thus leading to higher β values.

We also observe that S, previously associated with the particle's permeability, decreases when the continuous phase viscosity increases.

Here, higher viscosities are associated with higher polymer content: in such cases, the continuous phase goes through particles less easily, giving rise to lower apparent permeabilities

Adjustments of the model

This work highlights the interest of a model that goes beyond a constant random close packing defined for swollen particles. However, a clear limitation of the model is that Eq. (6) implies that a finite value of the critical volume fraction ϕ_c cannot be determined from a set of data, since it increases monotonically with the particle volume fraction : for different volume fractions ϕ, different values of ϕ_c are determined. Still, at sufficiently high concentrations, cells should become incompressible, and therefore, the volume fraction reaches a finite, maximum value. This maximum volume fraction, ϕ_{max}, is an important characteristic of a given system, as it gives a clear indication of the maximum compression level that can be reached physically, which should depend on the particles structure and composition. To circumvent this limitation, we propose to modify the existing model so that this maximum volume fraction could be included, as indicate in the following equation:

$$\phi_c = \phi_{rcp} + \frac{\phi_{max} - \phi_{rcp}}{1 + exp\left[-\Lambda\left(\phi_{app} - \phi_i\right)\right]} \quad (9)$$

As proposed by Mendoza, the critical volume fraction evolves here with the particle concentration above the random close packing volume fraction defined for hard spheres. However, rather than using a power law model, leading to an infinite critical volume fraction, we use a sigmoidal law, so that a finite maximal volume fraction (ϕ_{max}) will be reached eventually.

While this equation involves an additional variable, it seems more physically realistic to the vegetable particles of ours. As it includes a sigmoid function, it allows to model the viscosity evolution with volume fraction in a wider range of concentrations, including the divergence that should occur at extremely high volume fractions. The maximum attainable volume fraction ϕ_{max} included in Eq. (9) allows us to translate the incompressibility limit

encountered by the particles at high volume fraction, which, in our case, results in a divergence of the viscosity at high volume fraction, assuming that particles are not able to shrink or deform anymore. It is however less accurate for very diluted systems: for extremely low values of ϕ_{app}, the critical volume fraction ϕ_c remains slightly higher than ϕ_{rcp} in our model. Still, food suspensions are rarely highly diluted system and Einstein's law remains the best way to fit very diluted systems.

In Eq. (9), the model parameters can be associated with different physical properties. Λ defines the spreading of sigmoid (i. e., the slope of the sigmoid at the inflection point) and ϕ_i defines the value of the inflection point which corresponds to the points for which the particle compressibility towards particles concentration is maximum. The sigmoid is also defined by two asymptotes, the first one is equal to zero, and the second one is defined by the parameter ϕ_{max}. This parameter set the critical volume in a finite range between ϕ_{rcp} and ϕ_{max}, and allows the estimation of the latter from experimental data

To summarize, we fitted in Figure 7 our data with the most widely used models in the literature (i.e. the Einstein model, the Quemada model and the Krieger-Dougherty model), with the model proposed by Mendoza and with the model we propose here (combining equations (4), (5) and (9)). The parameters used to fit our data points are summarized in Table 4. The Einstein model, the only theoretical model describing the evolution of viscosity with the apparent volume fraction, does not allow to model concentrated systems. Thus, as expected, it does not fit our data over the entire range of concentrations studied. The Quemada and Krieger-Dougherty models also do not fit our data correctly, because in these models the viscosity increases more and more as the volume fraction increases, till it diverges at volume fractions much lower than the ones reached experimentally. The Mendoza model, as we have seen in this work, allows us to successfully model the entire range of concentration that was experimentally investigated. However, in this model the viscosity will continuously increases with the volume fraction, as an upper limit for ϕ_c will never be reached, whatever the value of ϕ. As it can be observed, the model we propose allows by contrast to fit the whole range of our data (from diluted to highly concentrated) while having a volume fraction upper limit.

490

491 *Table 4. Models used for the Figure 7*

Models	Equation and parameters used in Figure 7
Einstein	$\eta(\phi) = \eta_0(1 + k_E\phi)$ $k_E = 2.5$
Quemada	$\eta(\phi) = \eta_0\left(1 - \frac{\phi}{\phi_{rcp}}\right)^{-q}$ $q = 2.0\ ;\ \phi_{rcp} = 0.637$
Krieger-Dougherty	$\eta(\phi) = \eta_0\left(1 - \frac{\phi}{\phi_{rcp}}\right)^{-k_E\phi_{rcp}}$ $k_E = 2.5\ ;\ \phi_{rcp} = 0.637$
Mendoza	$\eta(\phi) = \eta_0\left(1 - \frac{\phi}{1 - k\phi}\right)^{-[\eta]}$ $k = \frac{1 - \phi_c}{\phi_c}\ ;\ \phi_c = \phi_{rcp} + \beta\phi^{\alpha}$ $\alpha = 1.964\ ;\beta = 0.851\ ;\ \phi_{rcp} = 0.637\ ;[\eta] = 3.226$
Current model	$\eta(\phi) = \eta_0\left(1 - \frac{\phi}{1 - k\phi}\right)^{-S}$ $k = \frac{1 - \phi_c}{\phi_c}\ ;\ \phi_c = \phi_{rcp} + \frac{\phi_{max} - \phi_{rcp}}{1 + \exp[-\Lambda(\phi - \phi_i)]}$ $\Lambda = 1.87\ ;\ \phi_i = 2.38\ ;\ \phi_{max} = 16\ ;\ \phi_{rcp} = 0.637\ ;S = 3.76$

492

493

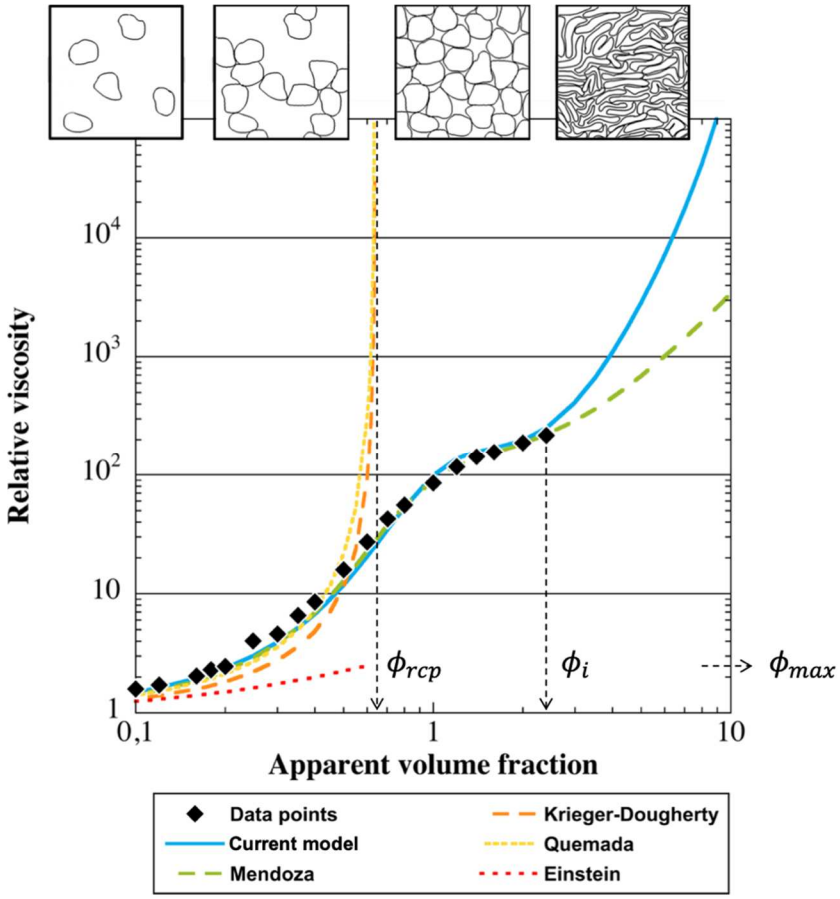

Figure 7. Modelling of model suspensions in apple serum with theoretical and phenomenological models describing the evolution of the viscosity with the apparent volume fraction. Model and parameter used are summarized in Table 4

Conclusion

In this work, an indirect way of accessing the effective volume fraction of the particles and a model describing the concentration dependence of the viscosity of soft plant cells suspensions over a wide range of concentration were proposed.

The model, initially proposed for soft colloidal particles and applied to star polymers[16], was successfully applied to real apple purees of several grindings and to monodispersed suspensions of apples cells in several continuous phases. Three adjustment parameters are defined and related to the particle's intrinsic physical properties: deformability, sphericity and porosity.

We also showed that for such non-colloidal suspensions, in which friction forces play an important role in the rheological properties, those parameters are also related to the continuous phase properties that may act as a lubricant and decrease frictional interactions.

To represent the predictable divergence of the viscosity at the maximum packing fraction, we successfully introduced a sigmoid-type term in the model, which allows the prediction of the viscosity in the entire range of volume fraction. This new model necessitates additional parameters, however these parameters now include a key characteristic of a compressible suspension, namely the maximum volume fraction, ϕ_{max}, that is reached when particles are fully compressed. For the system investigated here, we found ϕ_{max}=16, which demonstrates the extremely high compressibility of apple cells. This estimation calls for future work: investigating apple cells suspensions rheological properties in extremely concentrated states would allow to confirm the validity of the model in this limit. The predicted divergence of the viscosity while approaching ϕ_{max} indeed assumes that in this limit, particles become incompressible but also cannot deform anymore, which seems reasonable considering the high level of entanglement, but have not been confirmed experimentally to date to our knowledge Also, future work should be done on others food soft granular suspension to evaluate how this model could be applied to other systems.

This model represents a significant advance in the understanding of processed fruit and vegetables systems and offers clear industrial prospects.

We believe the attempt to link macroscopic behavior with local properties such as compressibility or friction in such systems would benefit from in-depth investigation at the particles scale, both experimentally and numerically, that would certainly in the future allow a better description of their behavior.

Acknowledgements

The research leading to these results has received funding from the European Union's Seventh Framework Programme for research, technological development and demonstration under grant agreement number 311754. The authors wish to thank Adeline Boire, for fruitful discussions.

References

1. Ubbink, J. Soft matter approaches to structured foods: from “cook-and-look” to

rational food design ? *Faraday Discuss.* **158**, 9 (2012).

2. Vilgis, T. A. Soft matter food physics—the physics of food and cooking. *Reports Prog. Phys.* **78**, 124602 (2015).

3. Sman, R. G. M. Van Der. Soft matter approaches to food structuring. *Adv. Colloid Interface Sci.* **176**–**177**, 18–30 (2012).

4. Boire, A. *et al.* Soft-Matter Approaches for Controlling Food Protein Interactions and Assembly. *Annu. Rev. Food Sci. Technol.* **10**, 521–542 (2019).

5. Lopez-Sanchez, P., Chapara, V., Schumm, S. & Farr, R. Shear Elastic Deformation and Particle Packing in Plant Cell Dispersions. *Food Biophys.* **7**, 1–14 (2012).

6. Leverrier, C., Almeida, G., Espinosa-Munoz, L. & Cuvelier, G. Influence of Particle Size and Concentration on Rheological Behaviour of Reconstituted Apple Purees. *Food Biophys.* **11**, 235–247 (2016).

7. Roversi, T. & Piazza, L. Supramolecular assemblies from plant cell polysaccharides: Self-healing and aging behavior. *Food Hydrocoll.* **54**, 189–195 (2016).

8. Chen, D. T. N., Wen, Q., Janmey, P. A., Crocker, J. C. & Yodh, A. G. Rheology of Soft Materials. *Annu. Rev. Condens. Matter Phys.* **1**, 301–322 (2010).

9. Seth, J. R., Mohan, L., Locatelli-Champagne, C., Cloitre, M. & Bonnecaze, R. T. A micromechanical model to predict the flow of soft particle glasses. *Nat. Mater.* **10**, 838–43 (2011).

10. Day, L., Xu, M., Øiseth, S. K., Lundin, L. & Hemar, Y. Dynamic rheological properties of plant cell-wall particle dispersions. *Colloids Surf. B. Biointerfaces* **81**, 461–467 (2010).

11. Espinosa-Muñoz, L., Renard, C. M. G. C., Symoneaux, R., Biau, N. & Cuvelier, G. Structural parameters that determine the rheological properties of apple puree. *J. Food Eng.* **119**, 619–626 (2013).

12. Schijvens, E. P. H. M., Van Vliet, T. & Van Dijk, C. Effect of processing conditions on the composition and rheological properties of applesauce. *J. Texture Stud.* **29**, 123–143 (1998).

13. Moelants, K. R. N. *et al.* Relation Between Particle Properties and Rheological Characteristics of Carrot-derived Suspensions. *Food Bioprocess Technol.* **6**, 1127–1143 (2013).

14. Day, L., Xu, M., Øiseth, S. K., Hemar, Y. & Lundin, L. Control of Morphological and Rheological Properties of Carrot Cell Wall Particle Dispersions through Processing.

Food Bioprocess Technol. **3**, 928–934 (2010).

15. Koumakis, N., Pamvouxoglou, A., Poulos, A. S. & Petekidis, G. Direct comparison of the rheology of model hard and soft particle glasses. *Soft Matter* **8**, 4271 (2012).
16. Mendoza, C. I. Model for the Shear Viscosity of Suspensions of Star Polymers and Other Soft Particles. *Macromol. Chem. Phys.* **214**, 599–604 (2013).
17. Leverrier, C., Almeida, G., Menut, P. & Cuvelier, G. Design of Model Apple Cells Suspensions: Rheological Properties and Impact of the Continuous Phase. *Food Biophys.* **12**, 383–396 (2017).
18. Müller, S. & Kunzek, H. Material properties of processed fruit and vegetables I . Effect of extraction and thermal treatment on apple parenchyma. *Zeitschrift für Leb. und - forsch. A* **206**, 264–272 (1998).
19. Espinosa, L. *et al.* Effect of processing on rheological, structural and sensory properties of apple puree. *Procedia Food Sci.* **1**, 513–520 (2011).
20. Espinosa, L. Texture de la purée de pomme : influence de la structure sur les propriétés rhéologiques et la perception sensorielle - effet du traitement mécanique. (AgroParisTech - Ingénierie Procédés aliments, 2012).
21. Shewan, H. M. & Stokes, J. R. Viscosity of soft spherical micro-hydrogel suspensions. *J. Colloid Interface Sci.* **442**, 75–81 (2015).
22. Boehm, M. W., Warren, F. J., Baier, S. K., Gidley, M. J. & Stokes, J. R. Food Hydrocolloids A method for developing structure-rheology relationships in comminuted plant-based food and non-ideal soft particle suspensions. *Food Hydrocoll.* **96**, 475–480 (2019).
23. Fernandez-Nieves, A., Wyss, H. M., Mattsson, J. & Weitz, D. A. *Microgel Suspensions Fundamentals and Applications*. (Wiley-VCH, 2011). doi:10.1017/CBO9781107415324.004
24. Batchelor, G. K. & Green, J. T. The determination of the bulk stress in a suspension of spherical particles to order c^2. *J. Fluid Mech.* **56**, 401–427 (1972).
25. Taylor, G. I. The viscosity of a fluid containing small drops of another fluid. *Proc. R. Soc. A Math. Phys. Eng. Sci.* **138**, 41–48 (1932).
26. Macosko, C. *Rheology: Principles, Measurements and Applications*. *Powder Technology* (Wiley-VCH, 1996). doi:10.1016/S0032-5910(96)90008-X
27. Silbert, L. Jamming of frictional spheres and random loose packing. *Soft Matter* **13**,

(2010).
28. Dong, K. J., Yang, R. Y., Zou, R. P. & Yu, A. B. Role of Interparticle Forces in the Formation of Random Loose Packing. *Phys. Rev. Lett.* **96**, (2006).
29. Mendoza, C. I. & Santamaría-Holek, I. The rheology of hard sphere suspensions at arbitrary volume fractions: An improved differential viscosity model. *J. Chem. Phys.* **130**, (2009).
30. Mendoza, C. I. & Santamaría-Holek, I. Rheology of concentrated emulsions of spherical droplets. *Appl. Rheol.* **20**, 1–3 (2010).
31. Santamaría-Holek, I. & Mendoza, C. I. The rheology of concentrated suspensions of arbitrarily-shaped particles. *J. Colloid Interface Sci.* **346**, 118–26 (2010).
32. Mendoza, C. I. Effective static and high-frequency viscosities of concentrated suspensions of soft particles. *J. Chem. Phys.* **135**, (2011).
33. Krieger, I. M. & Dougherty, T. J. A Mechanism for Non-Newtonian Flow in Suspensions of Rigid Spheres. *Trans. Soc. Rheol.* **III**, 137–152 (1959).
34. Adams, S., Frith, W. J. & Stokes, J. R. Influence of particle modulus on the rheological properties of agar microgel suspensions. *J. Rheol. (N. Y. N. Y).* **48**, 1195–1213 (2004).
35. Ellis, A. & Jacquier, J. C. Manufacture and characterisation of agarose microparticles. *J. Food Eng.* **90**, 141–145 (2009).
36. Quemada, D. *Modélisation rhéologique structurelle : dispersions concentrées et fluides complexes*. (Lavoisier, 2006).
37. Quemada, D. Rheology of concentrated disperse systems and minimum energy dissipation principle I . Viscosity-concentration relationship. *Rheol. Acta* **16**, 82–94 (1977).
38. Mueller, S., Llewellin, E. W. & Mader, H. M. The rheology of suspensions of solid particles. *Proc. R. Soc. A Math. Phys. Eng. Sci.* **466**, 1201–1228 (2010).
39. Farr, R. S. & Groot, R. D. Close packing density of polydisperse hard spheres. *J. Chem. Phys.* **131**, 244104 (2009).
40. Menut, P., Seiffert, S., Sprakel, J. & Weitz, D. A. Does size matter? Elasticity of compressed suspensions of colloidal- and granular-scale microgels. *Soft Matter* **8**, 156 (2012).
41. Denn, M. M. & Morris, J. F. Rheology of Non-Brownian Suspensions. *Annu. Rev. Chem. Biomol. Eng.* **5**, 203–28 (2014).

42. Ancey, C., Coussot, P. & Evesque, P. A theoretical framework for granular suspensions in a steady simple shear flow. *J. Rheol. (N. Y. N. Y).* 1673 (1999). doi:https://doi.org/10.1122/1.551067